

Innovative Fingerprint Enhancement: Exploring Finger GAN's Constrained Generation Scheme

- 1) Sahana D Gowda, Asst. Professor, Department of Computer Science and Engineering, BGSIT, ACU, Mandya
- 2) Manoj V, Department of Computer Science and Engineering, BGSIT, 20CSE044, ACU, Mandya

Abstract— Inert unique finger impression improvement is a fundamental pre-handling step for idle finger impression distinguishing proof. Most inactive finger impression improvement strategies attempt to reestablish ruined dim edges/valleys. In this paper, we propose another strategy that formulates dormant unique mark upgrade as an obliged finger impression age issue inside a generative ill-disposed network (GAN) structure. We name the proposed network FingerGAN. It can implement its created unique finger impression (i.e, improved idle balance gerprint) unclear from the relating ground truth case as far as the finger impression skeleton map weighted by particulars areas and the direction field regularized by the FOMFE model. Since details is the essential component for unique mark acknowledgment and particulars can be recovered straightforwardly from the finger impression skeleton map, we offer an all encompassing structure that can perform dormant finger impression upgrade with regards to straightforwardly streamlining particulars data. This will assist with further developing inactive finger impression ID execution essentially. Trial results on two public inactive finger impression data sets show that our technique beats the condition of artistic expressions altogether.

Index Terms—Constrained fingerprint generation, deep convolutional generative adversarial network, latent fingerprint enhancement.

I INTRODUCTION

FINGERPRINTS have been widely used for human verification and identification in many civil or criminal applications [1], [2].

Different from plain and rolled fingerprints that are acquired professionally, latent fingerprints refer to fingerskin impressions unintentionally left at a crime scene and are generally used as important evidence to identify criminals by law enforcement and forensic agencies. Compared with plain and rolled fingerprints, latent fingerprints are usually smudgy and blurred, with incomplete regions, unclear ridge structures,

Manuscript received 14 December 2021; revised 5 December 2022; accepted 7 January 2023. Date of publication 13 January 2023; date of current version 5 June 2023. This work was undertaken with the assistance of resources and services provided by National Computational Infrastructure (NCI) organization, which is supported by the Australian Government. This work was partially supported by ARC Discovery Grants under Grants DP190103660 and DP200103207 and in part by ARC Linkage under Grant LP180100663. Recommended for acceptance by J. Zhou. (*Corresponding author: Jiankun Hu.*)

Yanming Zhu is with the School of Computer Science and Engineering, University of New South Wales, Sydney, NSW 2052, Australia (e-mail: yanming.zhu@unsw.edu.au).

Xuefei Yin and Jiankun Hu are with the School of Engineering and Information Technology, University of New South Wales, Canberra, ACT 2600, Australia (e-mail: xuefei.yin@unsw.edu.au; J.Hu@adfa.edu.au).

Digital Object Identifier 10.1109/TPAMI.2023.3236876

and complex background noise. Due to these factors, the identification accuracy of latent fingerprints, which heavily relies on fingerprint quality, is much lower than that of plain and rolled fingerprints. Therefore, latent fingerprint enhancement, which aims to improve latent fingerprint quality, becomes one of the most necessary and important preprocessing steps for latent fingerprint identification.

Over the past few decades, many efforts have been made toward latent fingerprint enhancement [3], [4], [5], [6], [7]. In the early days, classical image processing techniques such as contextual filtering and directional filtering were introduced to enhance fingerprints. For example, Cappelli et al. [8] proposed tuning a Gabor filter to the local orientations and frequencies of fingerprints to suppress noise and improve the clarity of ridge structure. Chikkerur et al. [9] proposed performing contextual filtering in the Fourier domain to enhance fingerprints. However, these methods are mainly effective for bad-quality plain or rolled fingerprints, and tend to fail in latent fingerprint enhancement due to: 1) the corrupted ridge structures caused by structural noise in latent fingerprints; and 2) the unreliable orientation and frequency estimation caused by the low clarity of ridge structures of latent fingerprints. Therefore, varieties of smoothing and global modeling techniques were proposed to address the above problems and devoted to reliable orientation estimation to improve the latent fingerprint enhancement [10], [11], [12], [13]. For example, Yoon et al. [11] proposed using a polynomial model together with Gabor filters to estimate the fingerprint orientations to improve the latent enhancement. Feng et al. [12] proposed using an orientation patch dictionary to estimate orientations and then applying Gabor filtering to the orientations to achieve latent fingerprint enhancement. Yang et al. [13] proposed to further improve the above method by replacing its orientation dictionary with a set of localized orientation dictionaries. However, tuning of Gabor filters requires a fixed ridge frequency. This is problematic because the ridge frequency of fingerprints is not constant.

Later, to further improve the enhancement of latent fingerprints, various total variation (TV) image models, which minimize the total variation of an image and decompose the image into two components of texture and cartoon, were adopted to take advantage of ridge structures [14], [15], [16], [17]. For example, Zhang et al. firstly proposed an adaptive TV model [14] to remove the structural noise of latent fingerprints and then proposed an adaptive directional TV model [15] for latent fingerprint enhancement. These methods can restrain the

structural noise in the decomposed texture components of latent fingerprints by integrating local orientations and scales of fingerprints. However, estimating the local parameters of these models for poor-quality latent fingerprints is difficult and thus the extracted ridge structures by these models are usually weak. Therefore, in later research, TV decomposition is generally used as a preprocessing for latent fingerprint enhancement [16], [17].

After that, with the success of deep learning, deep neural networks were proposed for latent fingerprint enhancement [18], [19], [20]. For example, Svoboda et al. [21] proposed using a convolutional autoencoder to reconstruct latent fingerprints. Li et al. [22] proposed a deep convolutional network consisting of one convolution and two deconvolution parts for latent fingerprint enhancement. Qian et al. [23] proposed a latent fingerprint enhancement method based on DenseUnet. Horapong et al. [24] used a sparse autoencoder to boost the ridge/valley spectrum to enhance latent fingerprints. Liu et al. [25] proposed using deep nested UNets for latent fingerprint enhancement. These methods take advantage of the strong representation ability of deep neural networks and achieve remarkable results, but the corrupted ridge/valley structures of latent fingerprints are not well restored in most cases.

Recently, generative adversarial networks (GANs) have been used for latent fingerprint enhancement to enhance the restoration of ridge/valley structures. For example, Dabouei et al.

[26] proposed a conditional GAN for partial latent fingerprint enhancement, which achieves an enhancement of rejecting seriously corrupted fingerprint regions while improving ridge structure clarity in relatively good-quality regions. Joshi et al. [27] proposed a GAN-based algorithm to amplify the ridge/valley structure of latent fingerprint for enhancement. Huang et al.

[28] proposed using a progressive PatchGAN to achieve latent fingerprint enhancement. The enhancement ability of these methods mainly comes from the powerful feature representation and reconstruction ability of GANs.

In this paper, we propose a new method that formulates latent fingerprint enhancement as a constrained fingerprint generation problem within a GAN framework. The proposed network is named FingerGAN. It can enforce its generated fingerprint (i.e., enhanced latent fingerprint) indistinguishable from the corresponding ground truth instance in terms of the fingerprintskeleton map weighted by minutia locations and the orientationfield regularized by the FOMFE model. Because minutia is the primary feature for recognition and minutia can be retrieved directly from the fingerprint skeleton map [29], we offer a holistic framework that can perform latent fingerprint enhancement in the context of directly optimizing minutia information. This will help improve latent fingerprint identification performance significantly. Experimental results on two public latent fingerprint databases demonstrate that our method significantly outperforms the state of the arts.

The main contributions of this paper are summarized as follows.

- 1) Unlike most latent fingerprint enhancement methods that try to restore corrupted gray ridges/valleys, we propose a

new method that formulates latent fingerprint enhancement as a constrained fingerprint generation problem within a GAN framework.

- 2) We propose a FingerGAN which can generate enhanced latent fingerprints conditioned on a fingerprint-to-fingerprint translation and can enforce its generated enhanced latent fingerprints indistinguishable from the ground truth instances in terms of fingerprint skeleton map and orientation field.
 - 3) The fingerprint skeleton map is proposed as a ground truth because minutia is the primary feature for recognition and minutia can be retrieved directly from the fingerprint skeleton map. Also, a Gaussian-based minutia weight map is proposed to apply to the reconstruction loss, which can accommodate a moderate loss of the accuracy of minutia locations.
 - 4) The orientation field is proposed as a ground truth in a way of bringing in correspondence between the generated enhanced latent fingerprint and the ground truth orientation field. Also, the FOMFE model is adopted to regularize the orientation field so that the effects of spurious pixels and noise can be rectified.
 - 5) A synthetic latent fingerprint generation method is proposed, which can address the issue of lacking high-volume latent fingerprints and their true mates required for deep learning.
- The rest of this paper is organized as follows. Section II provides background information on related techniques. Section III describes the proposed method in detail. Section IV presents and discusses the experimental results. Finally, the paper is concluded in Section V.

II BACKGROUND

Since the proposed method involves GAN, U-Net, and the FOMFE fingerprint orientation model, relevant background knowledge is provided as follows.

A. Generative Adversarial Network

GAN is one of the most popular groups of generative networks, which learns to map an embedding space to a data distribution of interest, and has achieved great success in various image generation and processing tasks [26], [30], [31]. The underlying strategy of a GAN is emulating a competition, with a generative network, called generator G , which takes a random vector z sampled from a noise distribution Z as input and tries to generate samples as 'real' as possible, and a discriminative network, called discriminator D , which performs binary classification to distinguish samples generated by G from the real samples and acts as an adversary. The goal of G is to maximize the misclassification error of D while the goal of D is to beat G by learning to identify the generated samples. Through such a zero-sum game, the GANs have the ability to learn any kind of data distribution in an unsupervised manner. The networks of G and D are trained iteratively with two steps: 1) fixing the parameters of G and optimizing D ; and 2) fixing the parameters

of D and optimizing G by using a loss function formulated as [32]:

$$\min_G \max_D L(G, D) = \mathbb{E}_{x \in X} [\log(D(x))] + \mathbb{E}_{z \in Z} [\log(1 - D(G(z)))], \quad (1)$$

where x is the real sample from the data distribution X . $D(x)$ represents the binary classification score given input x . During the training, half of the samples are real and the rest $G(z)$ are samples generated by G given z .

Although the superiority of GAN in unsupervised representation learning, it can not be directly used for latent fingerprint enhancement due to its high probability of generating unrelated fingerprints. A GAN conditioned on the given information or constrained by prior knowledge can address this issue [31], [33], which inspires us to propose the FingerGAN. It is elaborately designed by customizing a GAN to fit the latent fingerprint enhancement task.

B. U-Net and Its Variations

U-Net [35] is a fully convolutional neural network (CNN) that was originally invented for biomedical image segmentation. It has a U-shaped encoder-decoder network architecture consisting of two main parts: a contracting path (encoder network) and an expansive path (decoder network). The encoder and decoder networks have four encoder blocks and four decoder blocks, respectively, and are connected via skip connections. The encoder network is responsible for feature extraction, which compresses the resolution of the input image and extracts target sensitive information. The decoder network is responsible for mixing the extracted features with the outputs of horizontally corresponding encoder blocks to generate a semantic segmentation mask. U-Net has been proven to be a powerful tool to learn efficient data presentation and semantically meaningful information. In fact, after this, the U-shaped network has been widely used in various tasks including image-to-image translation [31], [36]. Inspired by this, we propose embedding a U-shaped network in a GAN for latent fingerprint enhancement. It can leverage both the advantages of the U-shaped network and the advantages of GAN by jointly training the U-shaped network with an adversarial loss, as in [37].

C. FOMFE Model

FOMFE model describes the global topology of fingerprint ridges and is for modeling fingerprint orientations [38]. It is a regularized orientation field that is more reliable against noise and works well for low-quality fingerprints. Therefore, in this paper, we introduce it as prior knowledge to guide the constrained fingerprint generation.

III PROPOSED METHOD

A. Problem Formulation

We propose to formulate the latent fingerprint enhancement as a constrained fingerprint generation problem conditioned on a fingerprint-to-fingerprint translation. For this purpose, we

propose a FingerGAN by embedding a U-shaped network in a GAN such that the U-shaped network acts as the generator of the GAN, as illustrated in Fig. 1.

The U-shaped network is responsible for generating enhanced latent fingerprints given input latent fingerprints. Because minutia is the primary feature for recognition and minutia can be retrieved directly from the fingerprint skeleton map, we propose using the minutia location weighted fingerprint skeleton map as a ground truth to force the U-shaped network to perform latent fingerprint enhancement in the context of directly optimizing minutia information. The discriminator is used to force the U-shaped network to generate enhanced latent fingerprints indistinguishable from the ground truth instances in terms of both the fingerprint skeleton map and the FOMFE-based orientation field. For this purpose, its input is a concatenation¹ of the fingerprint skeleton map and the FOMFE-based orientation field. Specifically, the U-shaped network generated enhanced latent fingerprint and the ground truth orientation field are concatenated to form a type of input. The ground truth skeleton map and the ground truth orientation field are concatenated to form another type of input. The discriminator tries to distinguish these two types of inputs to beat the U-shaped network. This design of concatenation brings in correspondence between the generated enhanced fingerprint and the ground truth orientation field. Therefore, the generation of the U-shaped network is constrained by prior knowledge of FOMFE-based orientation field and can address the problem of generating unrelated fingerprints. Details of the proposed FingerGAN are provided in the following Section III.B.

B. Details of the Proposed FingerGAN

Fig. 2 illustrates the details of the proposed FingerGAN.

U-Shaped Network: The U-shaped network consists of an encoder with five composite convolutional blocks (C1-C5) and a decoder with five deconvolutional blocks (DC1-DC5), where skip connection [39] is adopted for the first four composite deconvolutional blocks. This is proposed to keep the high-frequency details of the inputs and increase the quality of the reconstruction from the decoder. Each of the first four composite convolutional blocks consists of two convolutional layers, and each convolutional layer is followed by a batch-normalization layer and a leaky rectified linear unit (ReLU) [40]. The last composite convolutional block consists of one convolutional layer, which is followed by a batch-normalization layer and a leaky ReLU layer. Each of the first four composite deconvolutional blocks consists of two up-convolutional layers, and each up-convolutional layer is followed by a batch-normalization layer and a leaky ReLU layer. The last composite deconvolutional block consists of an up-convolutional layer, a batch-normalization layer, and a sigmoid layer. According to the study in [41], successive convolutions by a set of small kernels are equal to one convolution by a larger kernel. It can effectively enhance a network's discriminative

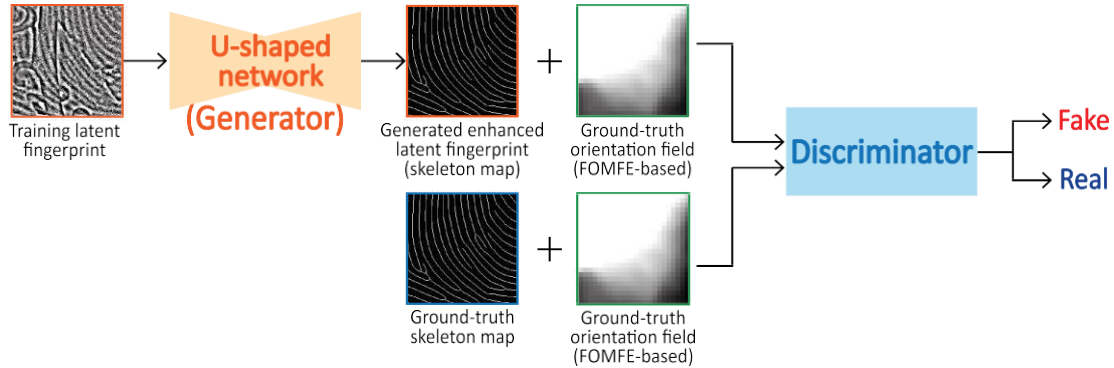


Fig. 1. The framework of the proposed FingerGAN. Texture components from the TV decomposition [34] are used as the latent fingerprints input to the U-shaped network because they are generally used as the representation of the latent fingerprints to be enhanced in current research [14], [15], [16], [17].

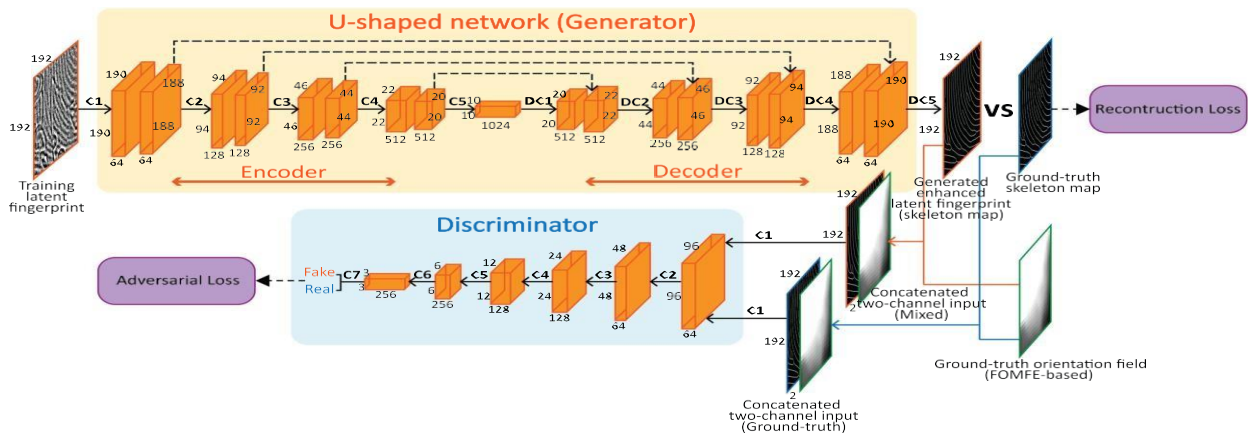


Fig. 2. Illustration of details of the proposed FingerGAN.

power and reduce the number of parameters required to be learned. In this paper, we use a set of small kernels and their details are reported in Table I. Also, we double or halve the kernel numbers when the size of feature maps halving or doubling.

The input of the U-shaped network is a latent fingerprint to be enhanced, and the output is the generated enhanced latent fingerprint. In the training stage, the input latent fingerprints are synthesized using rolled fingerprints by our proposed method described in the following Section III.C. The ground truths used to optimize the generation of the U-shaped network are the fingerprint skeleton maps of the rolled fingerprints. This way, by calculating a reconstruction loss between the generated enhanced latent fingerprint and the ground truth, the U-shaped network can learn to denoise the input latent fingerprint and reconstruct its fingerprint skeleton.

1) *Discriminator*: The architecture of the discriminator is a classical CNN. It has seven composite blocks, and each of the first six blocks consists of a convolutional layer followed by a batch-normalization layer and a leaky ReLU layer. The last

block consists of a convolutional layer, a batch-normalization layer, and a sigmoid layer. Similar to the parameter choice of the U-shaped network, we use small kernels for the discriminator. Details of the kernels are in Table I.

The discriminator takes a two-channel map as input and outputs a binary classification score. Specifically, the U-shaped network generated enhanced latent fingerprints and the ground truth skeleton map are respectively concatenated with the ground truth orientation field to form two types of two-channel inputs to the discriminator. The discriminator tries to distinguish them and thus can force the U-shaped network generated enhanced latent fingerprint indistinguishable from the ground truth in terms of the fingerprint skeleton map and the FOMFE-based orientation field. This way, it enables the U-shaped network to have an ability of deep semantic understanding, and thus to learn to restore the corrupted ridge structure of the latent fingerprint in addition to the denoising.

1) *Gaussian-Based Minutia Weight Map*: To force the U-shaped network to optimize minutia information, we propose a

TABLE I
DETAILS OF THE ARCHITECTURE OF
THE FINGERGAN

U-shaped network					Discriminator				
Block	Layer	Kernel Size	Stride	Kernel Number	Block	Layer	Kernel Size	Stride	Kernel Number
C1	conv1	3×3	1	64	DC1	up-conv1	2×2	2	512
	conv2	3×3	1	64		up-conv2	3×3	1	512
C2	conv1	2×2	2	128	DC2	up-conv1	2×2	2	256
	conv2	3×3	1	128		up-conv2	3×3	1	256
C3	conv1	2×2	2	256	DC3	up-conv1	2×2	2	128
	conv2	3×3	1	256		up-conv2	3×3	1	128
C4	conv1	2×2	2	512	DC4	up-conv1	2×2	2	64
	conv2	3×3	1	512		up-conv2	3×3	1	64
C5	conv1	2×2	2	1024	DC5	up-conv1	3×3	1	1

conv: convolution, up-conv: up-convolution.

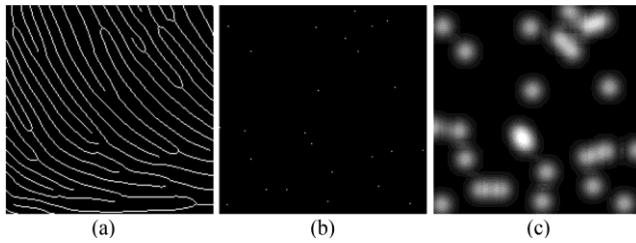


Fig. 3. Illustration of the proposed Gaussian-based minutia weight map. (a) a fingerprint skeleton map; (b) the minutia map M of (a); and (c) the Gaussian-based minutia weight map of (a).

Gaussian-based minutia weight map w which is defined as:

$$w(x, y) = \begin{cases} w^*(x, y), & \text{if } w^*(x, y) \neq 0, \\ 0, & \text{otherwise,} \end{cases} \quad (2)$$

with

$$w(x, y) = \frac{\sum_r \sum_{\substack{u=-r \\ v=-r}}^r wg(u, v) \cdot M(x+u, y+v)}{\sum_r \sum_{\substack{u=-r \\ v=-r}}^r wg(u, v)}, \quad (3)$$

$$wg(u, v) = \frac{1}{2\pi\sigma^2} e^{-\frac{u^2+v^2}{2\sigma^2}}, \quad (4)$$

and

$$w0 = \frac{\sum_r \sum_{\substack{u=-r \\ v=-r}}^r wg(r, r)}{\sum_r \sum_{\substack{u=-r \\ v=-r}}^r wg(u, v)}, \quad (5)$$

where (x, y) are coordinates of each pixel, (u, v) are coordinates of pixels in a local window centered at (x, y) , r is half the size of the local window, M is the minutia map whose value is 1 at minutia and 0 otherwise (as shown in Fig. 3b), and σ is the standard deviation of Gaussian. In the experiment, σ is set to be 8 and r is set to be 17. An example of the proposed weight maps is illustrated in Fig. 3.

4) Loss Functions: The FingerGAN has two losses: 1) an adversarial loss which is used to jointly train the discriminator and the U-shaped network, and force the U-shaped network to generate enhanced latent fingerprints indistinguishable from the ground truths in terms of fingerprint skeleton map and FOMFE-based orientation field; and 2) a reconstruction loss

which is used to further force the U-shaped network to generate enhanced latent fingerprints in the context of optimizing minutiae information.

Denote the training latent fingerprint as l and its domain as L , the U-shaped network as G , the generated enhanced latent fingerprint as $G(l)$, the ground truth skeleton map as g and its domain as G , the ground truth FOMFE-based orientation field as gF and its domain as GF [38], and the discriminator as D . According to the loss function in (1), the adversarial loss L_a is formulated as:

$$\min_G \max_D L_a(G, D) = \mathbb{E}_{g \in G, gF \in GF} [\log(D(g, gF))] + \mathbb{E}_{l \in L, gF \in GF} [\log(1 - D(G(l), gF))]. \quad (6)$$

We use the L1 loss as the reconstruction loss L_r , and thus it is formulated as:

$$L_r(G) = \mathbb{E}_{l \in L} [\|w \odot (g - G(l))\|_1], \quad (7)$$

where \odot denotes the element-wise multiplication. Overall, the total loss function is formulated as:

$$\min_G \max_D L = L_a + \eta L_r, \quad (8)$$

where η is a parameter that weights the contributions of the reconstruction loss and the adversarial loss. It is empirically set to be 0.001 in the experiments.

C. Proposed Training Data Generation

Applying deep learning to latent fingerprint applications is challenging because the current public databases either are short of the correspondence between latent fingerprints and their true mates or lack quantity. In this paper, we propose an effective procedure to generate the training data.

1) Overview: Fig. 4 illustrates the process of the proposed training data generation. First, a quality evaluation is performed on rolled reliable ground truth labels to provide meaningful supervision for the training. Then, the TV decomposition [34] is applied to those selected good-quality fingerprints to obtain their texture components, which are subsequently enhanced and thinned to generate ground truth skeleton

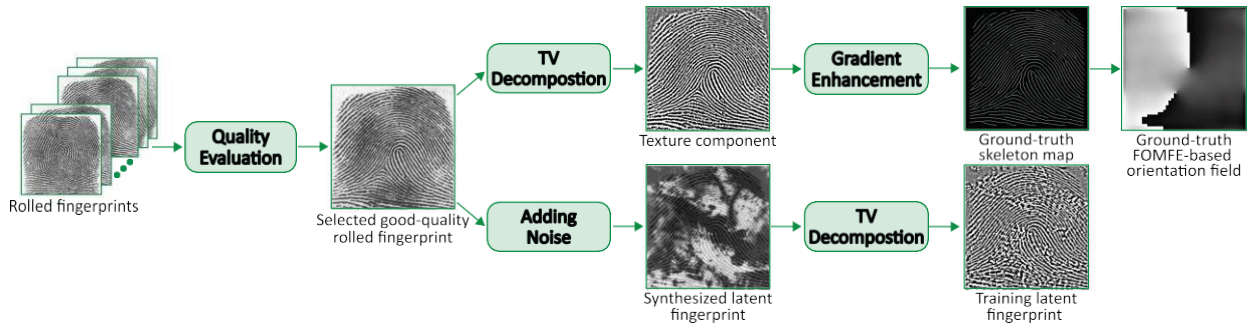


Fig. 4. Schematic diagram of the proposed training data generation.

maps. Also, ground truth FOMFE-based orientation fields are calculated based on the ground truth skeleton maps using the method in [38]. Meanwhile, noise is added to those selected good-quality fingerprints to obtain synthesized latent fingerprints, which are subsequently decomposed by the TV decomposition to obtain their texture components to be used as the training latent fingerprints. In the experiment, the rolled fingerprints are from the database NIST SD14 [42]. The quality evaluation is achieved using the method in [43] due to its effectiveness. The enhancement is achieved using the gradient-based method in [9] due to the good quality of those selected fingerprints. The noise is added by the proposed latent fingerprint synthesis method, which is described as follows.

2) *Latent Fingerprint Synthesis*: For better noise simulation, we propose adding complex and realistic noise instead of simple line or character noise adopted in previous works [18], [22]. This helps provide abundant training data that better mimics real latent fingerprint cases, and is important for the

U-shaped network to learn more effective representations of fingerprints from tough situations.

Given a selected rolled fingerprint b , firstly, a plastic distortion [44] is added by the following equation:

$$b_i^* = b_i + \Delta(b_i) \cdot g(h(b_i), k), \quad (9)$$

where $b_i = [x_i, y_i]^T$ is a point in b and b_i^* is its distorted point.

k is the skin plasticity coefficient. $\Delta(b_i)$ is the torsion and traction amount computed on the basis of a rotation angle ϑ and a displacement vector $e = [e_x, e_y]^T$, and is given by

$$\Delta(b_i) = (R\vartheta \cdot (b_i - o_r) + o_r + e) - b_i, \quad (10)$$

with

$$R\vartheta = \begin{bmatrix} \cos\vartheta & \sin\vartheta \\ -\sin\vartheta & \cos\vartheta \end{bmatrix}, \quad (11)$$

where

o_r is the center of rotation. $g(h(b_i), k)$ is the gradual transition defined as:

$$g(h(b_i), k) = \begin{cases} 0 & h(b_i) < 0 \\ \frac{1}{2} \frac{1 - \cos \frac{\pi \cdot h(b_i)}{k}}{2} & 0 < h(b_i) < k \\ 1 & \text{otherwise} \end{cases} \quad (12)$$

where function $h(b_i)$ returns a measure proportional to the distance between the point and the border of an ellipse centered

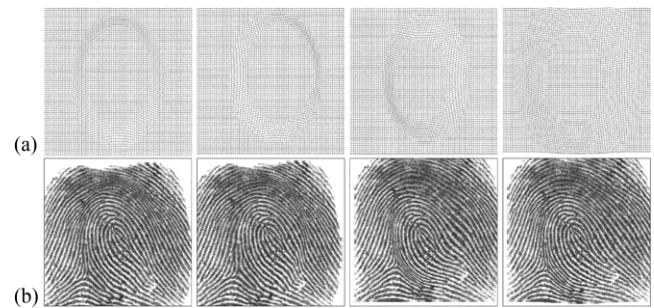


Fig. 5. Example of (a) various plastic distortions and (b) corresponding distorted fingerprints based on the same rolled fingerprint.

at o_e with semi-axes s_x and s_y , and is formulated as:

$$h(b_i) = \frac{1}{(b_i - o_e)^T A^{-1} (b_i - o_e)} - 1, \quad (13)$$

with

$$A = \begin{bmatrix} s_x^2 & 0 \\ 0 & s_y^2 \end{bmatrix} \quad (14)$$

In the experiments, to generate reasonable distortions, the ranges of values for parameters k , ϑ , e , and A are empirically set

(for s_y), respectively, where s is half of the size of the fingerprint image width. o_r and o_e are both set to be the center of the fingerprint image. Fig. 5 shows various plastic distortions and their corresponding distorted fingerprints based on the same rolled fingerprint.

Then, speckle noise is added to the distorted fingerprint b^* by the equation $b^{**} = b^* + n * b^*$, where n is uniformly distributed random noise with mean 0 and variance set to (0, 0.02). Finally, a latent fingerprint c is synthesized by fusing b^{**} and a realistic noise image d according to the equation:

$$c = (1 - \lambda)b^{**} + \lambda d, \quad (15)$$

where d is randomly cropped from the background regions of

latent fingerprints in the NIST SD27 database [42]. λ is a weight that measures the intensity degree of the realistic noise image.

In the experiments, its value ranges from 0.2 to 0.8. Fig. 6 shows some synthesized latent fingerprints and their training latent

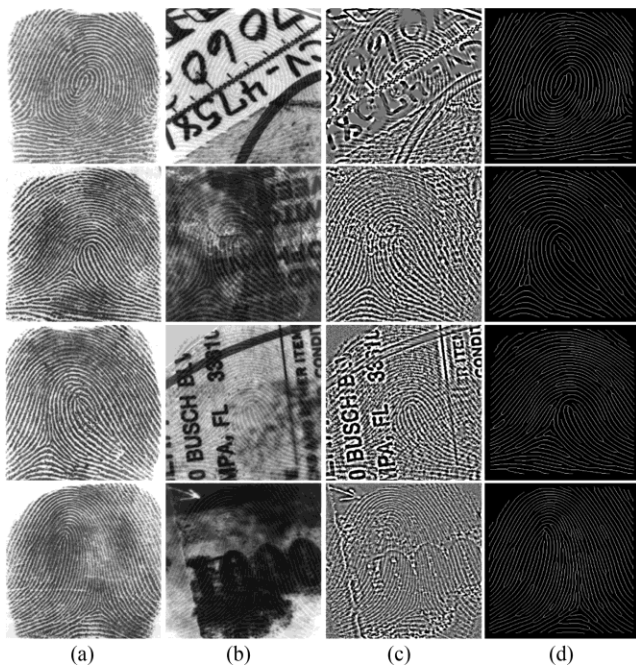


Fig. 6. Examples illustrating the proposed training data generation by (a) selected good-quality rolled fingerprints, (b) synthesized latent fingerprints of (a), (c) training latent fingerprints (TV decomposed textures) of (a), and (d) ground truth skeleton maps of (a).

fingerprints and ground truth skeleton maps generated by the proposed latent fingerprint synthesis method.

IV EXPERIMENTAL RESULTS

In this section, we evaluate our proposed method. Database and implementation details are firstly introduced in Section IV.A. Experimental results are then presented in Sections IV.B and IV.C. Finally, the proposed method is analyzed and discussed in Section IV.D.

A. Database and Implementation Details

1) **Database: Training Database** The database NIST SD14 [42] is used to generate the training data, which consists of 54,000 rolled fingerprint. According to the described method in Section III.C, a total of 13,000 good-quality fingerprints are selected from them. For each of the selected fingerprints, 10 latent fingerprints are synthesized, and thus the final training database consists of a total of 130,000 training latent fingerprints and 13,000 corresponding ground truth skeleton maps.

Test Databases Two challenging latent fingerprint databases NIST SD27 [45] and IIIT-Delhi MOLF [46] are used to evaluate the performance of the proposed method. Database NIST SD27 is provided by the National Institute of Standards and Technology in collaboration with the FBI. It contains 258 latent fingerprints collected from crime scenes, which are classified based on three different qualities, ‘good’, ‘bad’, and ‘ugly’, with numbers of images 88, 85, and 85, respectively. Latent fingerprints in this database contain complex noises and degradation of various types and levels, and therefore is a rigorous

benchmark for evaluating the performance of the proposed method. Database IIIT-Delhi MOLF is provided by Sankaran et al. and is widely used in latent fingerprint tasks in recent years. It contains 4,400 latent fingerprints and three sets of live-scan fingerprints obtained by different acquisition sensors of ‘Crossmatch’, ‘Secugen’, and ‘Lumidigm’. Each set has 4,000 live-scan fingerprints and can be used as a reference database for latent fingerprint identification. These three reference databases are denoted as ‘C’, ‘S’, and ‘L’, respectively. The resolution of images in these two databases is 500 ppi.

2) **Implementation Details: Enhancement.** Details of the architecture of the FingerGAN are provided in Fig. 2 and Table I. It was implemented in PyTorch and its optimizations are solved by the SGD solver Adam [47] with a learning rate of 0.001. During the training, 192×192 patches are used to train the FingerGAN. During the testing, for a latent fingerprint to be enhanced, a sliding window of size 192×192 with a step size of 8 was adopted to generate the enhanced latent fingerprint using the trained U-shaped network. Implementation codes will be available for non-commercial purposes from <https://github.com/HubYZ/LatentEnhancement>.

Identification. Enhanced latent fingerprint identification experiments are conducted to quantitatively evaluate the performance of the proposed method. For experiments conducted on the NIST SD27 database, the manually marked regions of interest provided in [12] are used consistently for all compared methods. Also, to make the identification more challenging, the reference fingerprint database is extended by adding rolled fingerprints from the NIST SD14 database. This is reasonable because the NIST SD14 database has been only used for enhancement training and has not been used in any way for the identification task. Therefore, each enhanced latent fingerprint is compared with a total of 27,258 rolled fingerprints for the identification. For experiments conducted on the IIIT-Delhi MOLF database, each enhanced latent fingerprint is compared with the first and second fingerprint samples of each subject for each of the three reference databases according to the test protocol established by Sankaran et al. [46]. The commercial software Neurotechnology VeriFinger SDK12.1² is used for the identification. The Cumulative Match Characteristic (CMC) curve is employed to evaluate the performance of the latent fingerprint identification.

B. Minutia Recovery Accuracy

1) **Quantitative Evaluation:** To evaluate the performance of our proposed method, we investigate our minutia recovery accuracy and compare it with those of the state-of-the-art Tang’s method [19], Qian’s method [23], Cao’s method [48], and Huang’s method [28]. This experiment is conducted on the NIST SD27 database because it provides manually marked minutiae which can be used as genuine minutiae. Recovered minutiae of each compared method are extracted using the VeriFinger12.1 from its enhanced

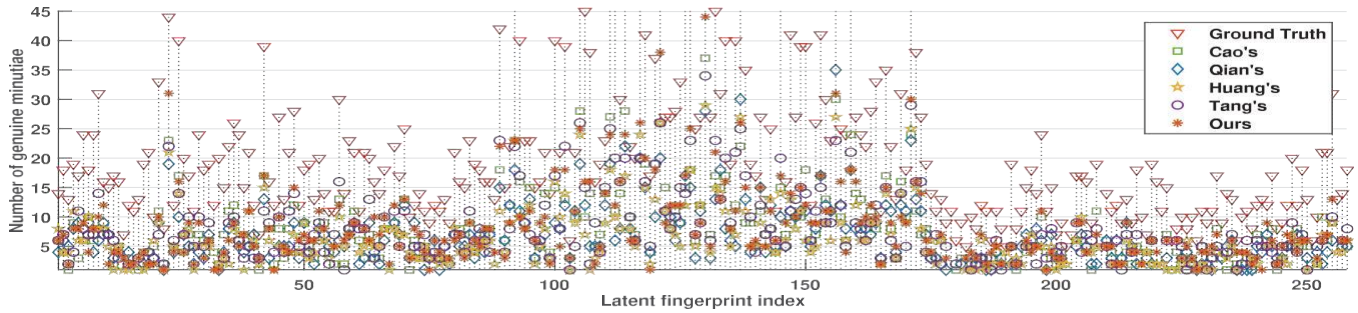


Fig. 7. Numbers of recovered genuine minutiae extracted from the enhanced latent fingerprints generated by our and the four compared methods, compared with the numbers of manually marked minutiae for each of the 258 latent fingerprints in the NSIT SD27 database.

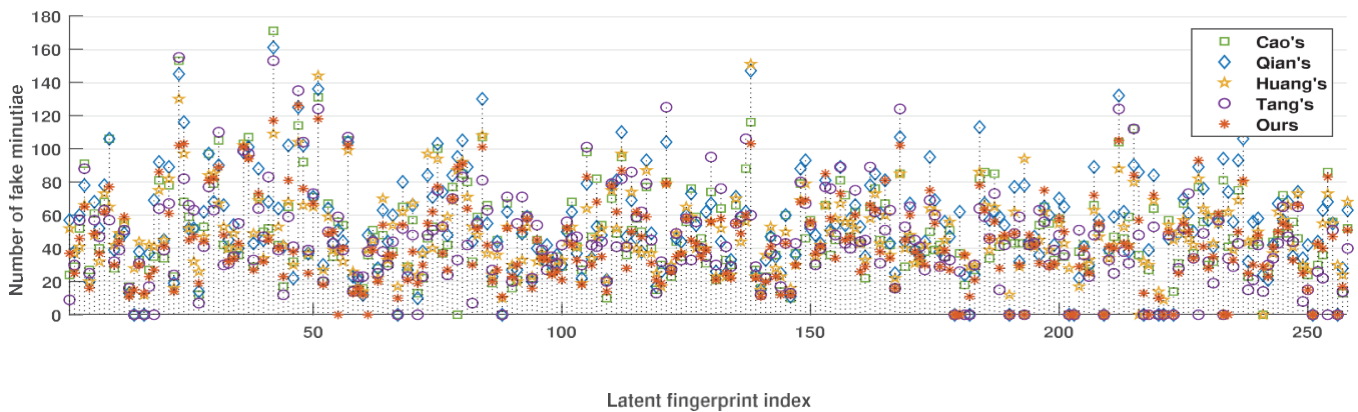


Fig. 8. Comparison of numbers of introduced fake minutiae in the enhanced latent fingerprints generated by our and the four compared methods for each of the 258 latent fingerprints in the NSIT SD27 database.

TABLE II
COMPARISON OF MINUTIA RECOVERY ACCURACY OF DIFFERENT METHODS IN TERMS OF OVERALL NUMBERS OF RECOVERED GENUINE MINUTIAE AND INTRODUCED FAKE MINUTIAE FOR THE 258 LATENT FINGERPRINTS IN THE NIST SD27 DATABASE

Method \ Metric	Recovered genuine minutiae	Introduced fake minutiae
Cao's	1,887	12,235
Qian's	1,631	13,985
Huang's	1,581	12,358
Tang's	1,919	11,579
Ours	1,982 1,982	11,152 11,152

latent fingerprints. We compare the extracted minutiae with the manually marked minutiae and define the recovered genuine minutiae as those extracted minutiae with both correct location, orientation, and minutia type in accordance with the manually marked minutiae. All the other extracted minutiae are defined as introduced fake minutiae. As can be seen from the results in Table II, our method achieves the best result, recovering more

genuine minutiae meanwhile introducing fewer fake minutiae than all the other methods.

Also, we provide a detailed comparison of the minutiae recovery accuracy of our and the four compared methods on

each of the 258 enhanced latent fingerprints in Figs. 7 and 8. As can be seen, compared with the second-best method (Tang's method), there are 112 latent fingerprints where our enhanced latent fingerprints recover more genuine minutiae, while there are 98 latent fingerprints where Tang's enhanced latent fingerprints recover more genuine minutiae than ours.

Furthermore, there are 128 latent fingerprints where our enhanced latent fingerprints introduce fewer fake minutiae than Tang's, while there are 111 latent fingerprints where Tang's enhanced latent fingerprints introduce fewer fake minutiae than ours. These results demonstrate the superiority of our method in terms of minutia recovery accuracy, and support our claim that the FingerGAN can perform latent fingerprint enhancement in the context of directly optimizing minutia information.

2) *Visual Inspection:* We provide an illustrative example in Fig. 9 for visually comparing the enhanced latent fingerprint of our and the four compared methods. Recovered minutiae are also labeled to compare with the manually marked minutiae. By observing and comparing the bottom right areas (yellow

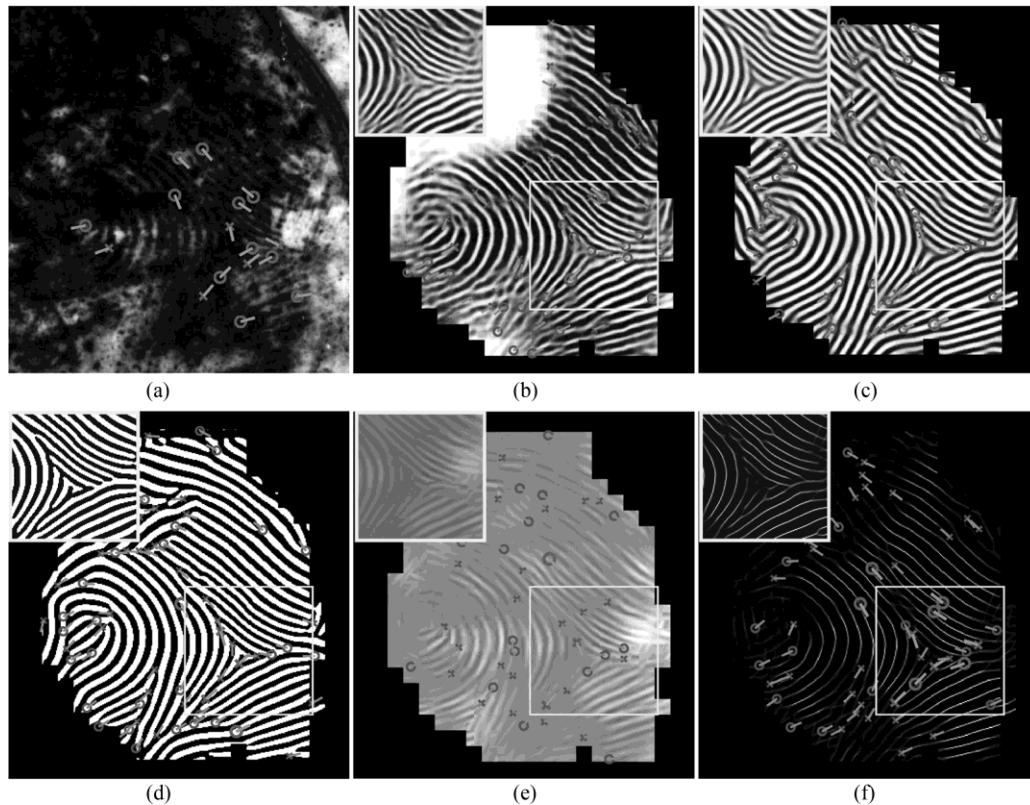


Fig. 9. Example of the comparison of the enhanced latent fingerprints generated by different methods. (a) Latent fingerprint B176 from the NIST SD27 database with the manually marked minutiae labeled as red circles or crosses, (b) the enhanced latent fingerprint by Cao's method, (c) the enhanced latent fingerprint by Qian's method, (d) the enhanced latent fingerprint by Huang's method, (e) the enhanced latent fingerprint by Tang's method, and (f) the enhanced latent fingerprint by our method. Recovered genuine minutiae and introduced fake minutiae in (b-f) are labeled as red and blue circles or crosses, respectively. Some regions of interest are highlighted in red rectangles.

rectangles) of the fingerprints in Fig. 9(b-f), we can observe that our enhanced latent fingerprint (f) gets better ridge/valley structures than the enhanced latent fingerprints (b-e) of the four compared methods. The superiority of our method can also be proved by observing the recovered genuine minutiae in Fig. 9(b-f). As can be seen, a total of 16 minutiae is manually marked in the latent fingerprint (a), only three, four, five, and three recovered genuine minutiae are extracted from Cao's, Qian's, Huang's, and Tang's enhanced latent fingerprints (b-e), respectively. However, ten recovered genuine minutiae are extracted from our enhanced latent fingerprint (f).

C. Identification Performance

1) *Evaluation on Database NIST SD27*: To comprehensively evaluate our proposed method, we perform fingerprint identification using our enhanced latent fingerprints and compare its performance with those achieved using enhanced latent fingerprints of the state-of-the-art Tang's method [19], Dabouei's method [49], Qian's method [23], Joshi's method [27], Cao's method [48], and Huang's method [28]. We conduct comparison experiments on all latent fingerprints, the 'good' latent fingerprints, the 'bad' latent fingerprints, and the 'ugly' latent fingerprints, respectively. Comparison results are shown in Fig. 10. As can be seen, our method achieves significantly better results than

all the other methods on the overall, the 'good', and the 'bad' latent fingerprints. For the identification on the 'ugly' latent fingerprints, our method achieves the tied best rank-1 result with Tang's method, and outperforms Tang's method in rank-2. These results demonstrate the superiority of our method in latent fingerprint enhancement.

2) *Evaluation on Database IIIT-Delhi MOLF*: We also compare the identification performance of using our enhanced latent fingerprints with those of using enhanced latent fingerprints of the six state-of-the-art methods (Tang's [19], Dabouei's [49], Qian's [23], Joshi's [27], Cao's [48], and Huang's [28] methods) on the IIIT-Delhi MOLF database. Fig. 11 shows the comparison of CMC curves achieved over the three reference databases 'C', 'S', and 'L', respectively. As can be seen, our method achieves consistently the best rank-1 performance over the three reference databases, which demonstrates the superiority and robustness of our method.

D. Ablation Study

To further analyze our method and justify the effectiveness of the FingerGAN design, we conduct the following ablation studies. These experiments are conducted on the NIST SD27 database using a reference database consisting of 258 corresponding rolled fingerprints of the NIST SD27 database. All

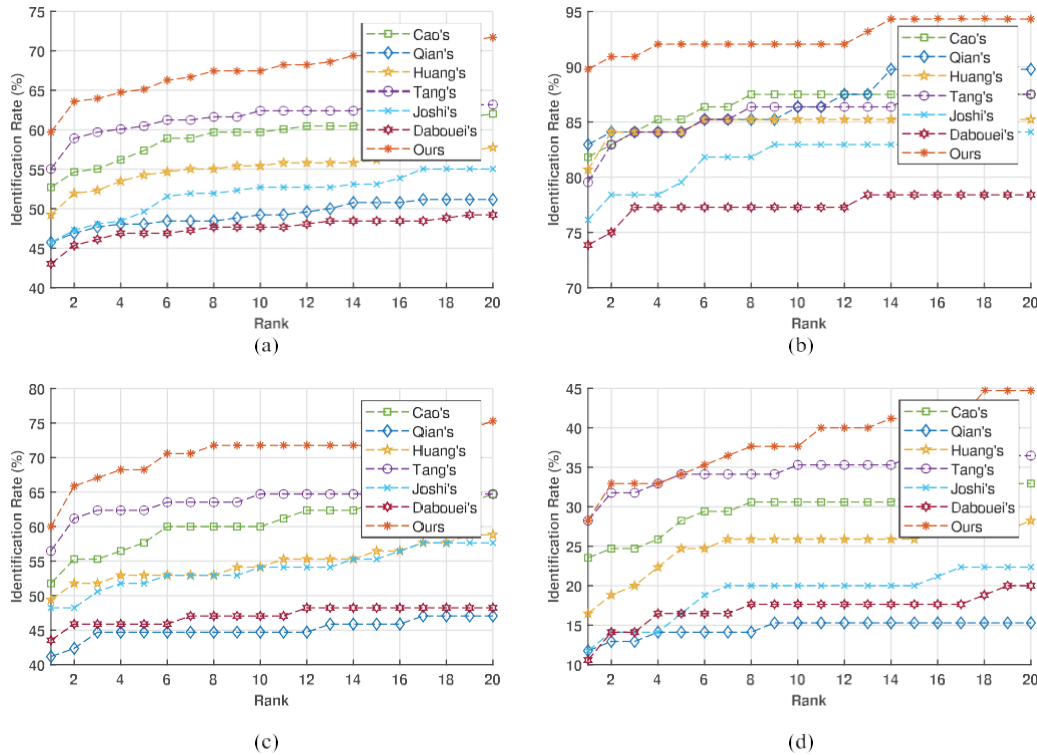


Fig. 10. Comparison of CMC curves achieved using the enhanced latent fingerprints generated by Cao's, Qian's, Huang's, Tang's, Joshi's, Dabouei's, and our methods on the NIST SD27 database. (a) CMC curves achieved using all latent fingerprints, (b) CMC curves achieved using the 'good' latent fingerprints, (c) CMC curves achieved using the 'bad' latent fingerprints, and (d) CMC curves achieved using the 'ugly' latent fingerprints.

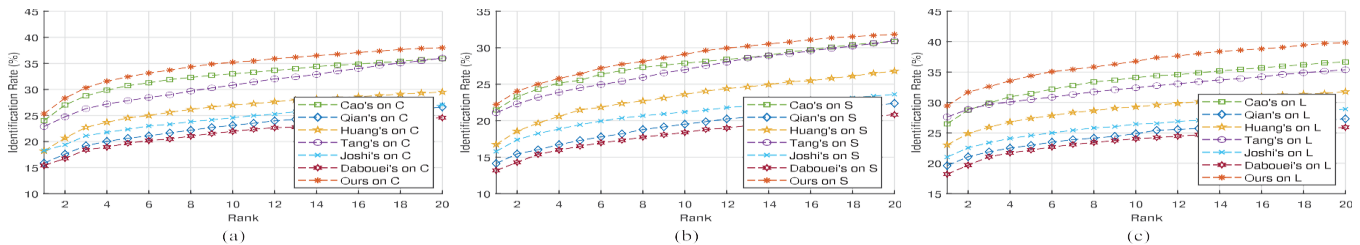


Fig. 11. Comparison of CMC curves achieved using the enhanced fingerprints generated by Cao's, Qian's, Huang's, Tang's, Joshi's, Dabouei's, and our methods on the IIIT-Delhi MOLF database over the three reference databases (a) 'C', (b) 'S', and (c) 'L', respectively.

other experimental settings are the same as those described in Section IV.A.2, except stated otherwise.

1) *The Advantage of Embedding the U-Shaped Network in a GAN:* To demonstrate the effectiveness of embedding the U-shaped network in a GAN, we conduct the following ablation study. We use only the proposed U-shaped network for latent fingerprint enhancement without using the discriminator, and name this method FingerGAN-noDiscriminator. Specifically, we train the U-shaped network using only the reconstruction loss in (7) with only the fingerprint skeleton maps as the ground truths. Fig. 12 compares the CMC curves achieved using the proposed FingerGAN and the FingerGAN-noDiscriminator. As can be seen, the rank-1 accuracy achieved using the FingerGAN (76.36%) is significantly higher than that achieved using the FingerGAN-noDiscriminator (70.54%). This demonstrates the

effectiveness of embedding the U-shaped network in a GAN and supports our claim that the proposed FingerGAN can force its generated enhanced latent fingerprints indistinguishable from the ground truths.

In addition, we provide an illustrative example in Fig. 13 for visually inspecting the enhanced latent fingerprints generated by the two models. As can be seen, the enhanced fingerprint generated by the FingerGAN is richer in ridge/valley details than that generated by the FingerGAN-noDiscriminator, as shown in the zoomed rectangles. This also results in more genuine minutiae being extracted from the enhanced latent fingerprint generated by the FingerGAN. This can be explained by the fact that the FingerGAN-noDiscriminator has only the L_r loss, which makes it focus only on the overall error of the corresponding pixels of the enhanced latent fingerprint and the

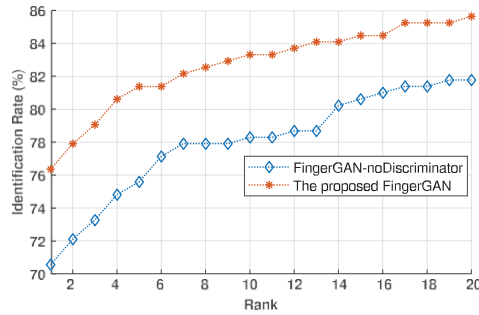


Fig. 12. Comparison of CMC curves achieved using the proposed FingerGAN and the FingerGAN-noDiscriminator.

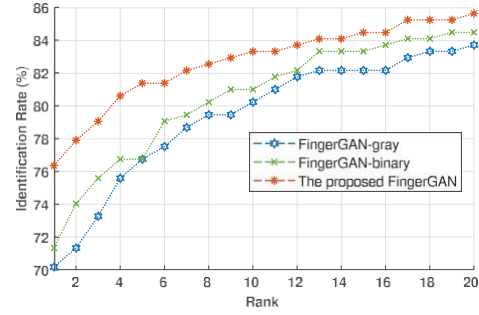


Fig. 14. Comparison of CMC curves achieved using FingerGAN-gray, FingerGAN-binary, and the proposed FingerGAN.

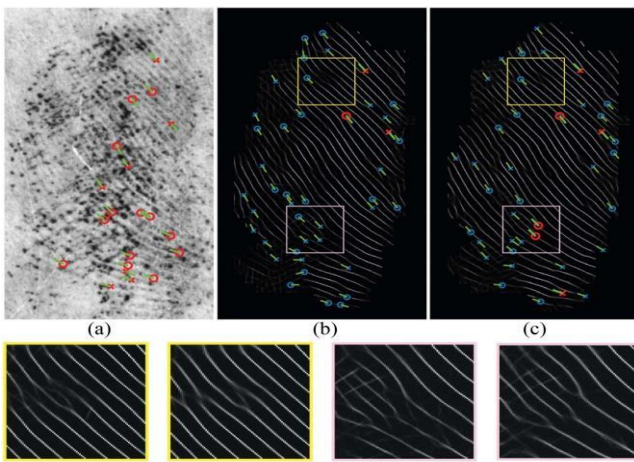


Fig. 13. Example of the comparison of the enhanced latent fingerprints generated by the FingerGAN-noDiscriminator and the FingerGAN. (a) Latent fingerprint U288 from the NIST SD27 database, where the manually marked minutiae are labeled as red circles or crosses, (b) and (c) enhanced latent fingerprints generated by FingerGAN-noDiscriminator and the FingerGAN, respectively, where the recovered genuine minutiae are labeled as red circles or crosses, and introduced fake minutiae are labeled as blue circles or crosses. Some regions of interest are highlighted in zoomed rectangles.

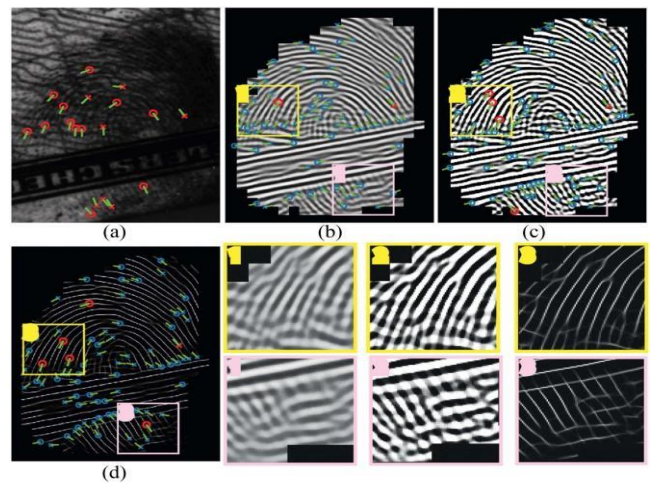


Fig. 15. Example of the comparison of the enhanced latent fingerprints generated by the FingerGAN-gray, FingerGAN-binary, and the FingerGAN. (a) Latent fingerprint U255 from the NIST SD27 database, where the manually marked minutiae are labeled as red circles or crosses, (b), (c), and (d) enhanced latent fingerprints generated by FingerGAN-gray, FingerGAN-binary, and the FingerGAN, respectively, where the recovered genuine minutiae are labeled as red circles or crosses, and introduced fake minutiae are labeled as blue circles or crosses. Some regions of interest are highlighted in zoomed rectangles.

ground truth, while the FingerGAN has an additional L_a loss to force the overall pattern of the enhanced latent fingerprint indistinguishable from that of the ground truth. It is well known that minutiae are salient features of fingerprints. They will affect fingerprint distinguishability significantly. Therefore, with the discriminator, the FingerGAN can facilitate better ridge/valley reconstruction, leading to better minutiae details.

2) *The Advantage of Using the Skeleton Map:* To demonstrate the effectiveness of using the fingerprint skeleton map as ground truth, we conduct the following ablation studies. We use fingerprint gray images and binary images instead of fingerprint skeleton maps as the ground truths respectively to train the FingerGAN, and name these two methods FingerGAN-gray and FingerGAN-binary respectively. Fig. 14 compares the CMC curves achieved using the proposed FingerGAN, the FingerGAN-gray, and the FingerGAN-binary. As can be seen,

the rank-1 accuracy achieved using the proposed FingerGAN (76.36%) is significantly higher than those achieved using the FingerGAN-gray (70.15%) and FingerGAN-binary (71.32%). This demonstrates the effectiveness of using the fingerprint skeleton map as ground truth and supports our claim that the skeleton map facilitates ridge/valley reconstruction.

In addition, we provide an illustrative example in Fig. 15 for visually inspecting the enhanced latent fingerprints generated by these three models. As can be seen, compared with the enhanced fingerprint generated by the FingerGAN-gray and FingerGAN-binary, the one generated by FingerGAN is much clearer in ridges/valleys, as shown in the zoomed rectangles, resulting in more minutiae being identified from it. This can be explained by the fact that minutia is defined on the skeleton map [29], thus using the skeleton map as the ground truth can directly

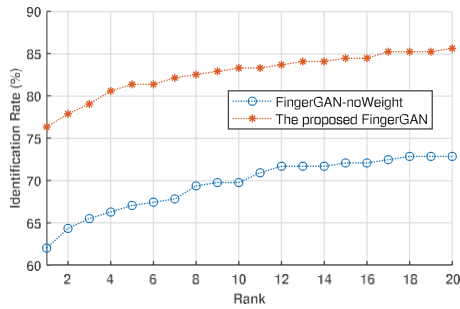


Fig. 16. Comparison of CMC curves achieved using the proposed FingerGAN and the FingerGAN-noWeight.

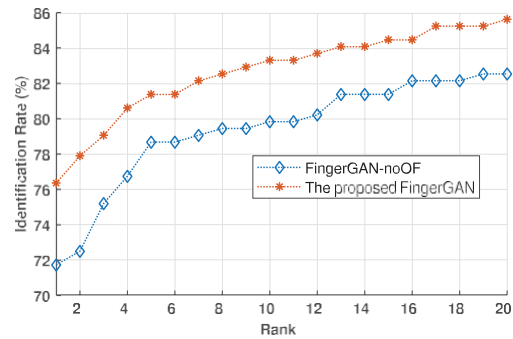


Fig. 18. Comparison of CMC curves achieved using the proposed FingerGAN and the FingerGAN-noOF.

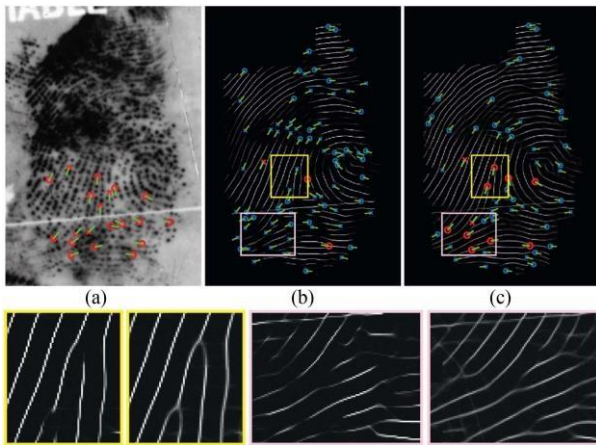


Fig. 17. Example of the comparison of the enhanced latent fingerprints generated by the FingerGAN-noWeight and the FingerGAN. (a) Latent fingerprint B164 from the NIST SD27 database, where the manually marked minutiae are labeled as red circles or crosses, (b) and (c) enhanced latent fingerprints generated by FingerGAN-noWeight and the FingerGAN, respectively, where the recovered genuine minutiae are labeled as red circles or crosses, and introduced fake minutiae are labeled as blue circles or crosses. Some regions of interest are highlighted in zoomed rectangles.

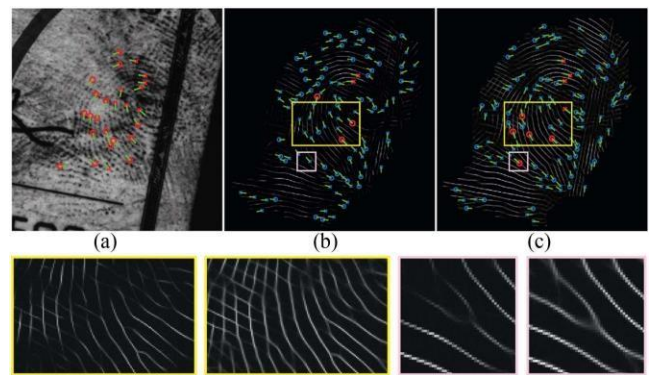


Fig. 19. Example of the comparison of the enhanced latent fingerprints generated by the FingerGAN-noOF and the FingerGAN. (a) Latent fingerprint B142 from the NIST SD27 database, where the manually marked minutiae are labeled as red circles or crosses, (b) and (c) enhanced latent fingerprints generated by FingerGAN-noOF and the FingerGAN, respectively, where the recovered genuine minutiae are labeled as red circles or crosses, and introduced fake minutiae are labeled as blue circles or crosses. Some regions of interest are highlighted in zoomed rectangles.

optimize the skeleton map of the enhanced latent fingerprint, leading to more accurate minutiae recovery.

3) *The Advantage of the Gaussian Minutia Weight:* To demonstrate the effectiveness of using the Gaussian-based minutia weight map, we conduct the following ablation study. We train the FingerGAN using a loss function without the Gaussian-based minutia weight map and name this method FingerGAN-noWeight. That is, we remove w in the (7) and make the reconstruction loss as $L_r(G) = E/l \in L[||g - G(l)||_1]$ to train the FingerGAN. Fig. 16 compares the CMC curves achieved using the proposed FingerGAN and the FingerGAN-noWeight. As can be seen, the rank-1 accuracy achieved using the proposed FingerGAN (76.36%) is significantly higher than that achieved using the FingerGAN-noWeight (62.02%). This demonstrates the effectiveness of using the Gaussian-based minutia weight map and supports our claim that the FingerGAN can perform latent fingerprint enhancement in the context of optimizing minutia information.

In addition, we provide an illustrative example in Fig. 17 for visually inspecting the enhanced latent fingerprints generated by the two models. As can be seen, the enhanced

fingerprint generated by the FingerGAN obtains better ridge/valley reconstruction, especially around minutiae, as shown in the zoomed rectangles. This results in obviously more minutiae being identified from it. This can be explained by the fact that the weighted reconstruction loss L_r forces the network to focus on the reconstruction of the weighted areas.

4) *The Advantage of Using Orientation Field:* To demonstrate the effectiveness of using the FOMFE-based orientation field, we conduct the following ablation study. We train the FingerGAN without using the FOMFE-based orientation field and name this method FingerGAN-noOF. Fig. 18 compares the CMC curves achieved using the proposed FingerGAN and the FingerGAN-noOF. As can be seen, the rank-1 accuracy achieved using the proposed FingerGAN (76.36%) is significantly higher than that achieved using the FingerGAN-noOF (71.72%). This demonstrates the effectiveness of using the FOMFE-based orientation field and supports our claim that the FOMFE-based orientation field acts as an additional constraint to guide the generation of enhanced latent fingerprints.

In addition, we provide an illustrative example in Fig. 19 for visually inspecting the enhanced latent fingerprints generated by the two models. As can be seen, the enhanced fingerprint

generated by the FingerGAN is better in ridge/valley details than that generated by the FingerGAN-noOF, as shown in the zoomed rectangles. This results in more genuine minutiae being extracted from the enhanced latent fingerprint generated by the FingerGAN. This can be explained by the fact that the FingerGAN-noOF has only the skeleton map constraint, while the FingerGAN incorporates an additional orientation constraint to make the enhanced latent fingerprint generation more constrained and more reliable.

V CONCLUSION

This paper proposed a FingerGAN for latent fingerprint enhancement, which formulates latent fingerprint enhancement as a constrained fingerprint generation problem. It can enforce its generated enhanced latent fingerprint indistinguishable from the corresponding ground truth instance in terms of the fingerprint skeleton map weighted by minutia locations and the orientation field regularized by the FOMFE model. Because minutia is the primary feature for recognition and minutia can be retrieved directly from the fingerprint skeleton map, we offer a holistic framework that can perform latent fingerprint enhancement in the context of directly optimizing minutia information. This will help improve latent fingerprint identification performance significantly. Experimental results on two public latent fingerprint databases demonstrate that our method outperforms the state of the arts significantly.

REFERENCES

- [1] M. Hawthorne, *Fingerprints: Analysis and Understanding*. Boca Raton, FL, USA: CRC, 2008.
- [2] D. Maltoni, D. Maio, A. K. Jain, and S. Prabhakar, *Handbook of Fingerprint Recognition*. 2nd ed., Berlin, Germany: Springer, 2009.
- [3] C. Wallace-Kunkel, C. Roux, C. Lennard, and M. Stoilovic, "The detection and enhancement of latent fingerprints on porous surfaces—a survey," *J. Forensic Identification*, vol. 54, no. 6, 2004, Art. no. 687.
- [4] A. Sankaran, M. Vatsa, and R. Singh, "Latent fingerprint matching: A survey," *IEEE Access*, vol. 2, pp. 982–1004, 2014.
- [5] A. V. Malwade, R. D. Raut, and V. Thakare, "A survey on fingerprint enhancement techniques using filtering approach," *Int. J. Electron. Commun. Soft Comput. Sci. Eng.*, 2015, Art. no. 372.
- [6] P. Schuch, S. Schulz, and C. Busch, "Survey on the impact of fingerprint image enhancement," *IET Biometrics*, vol. 7, no. 2, pp. 102–115, 2018.
- [7] B. Abebe, H. C. A. Murthy, E. Amare Zereffa, and Y. Dessie, "Latent fingerprint enhancement techniques: A review," *J. Chem. Rev.*, vol. 2, no. 1, pp. 40–56, 2020.
- [8] R. Cappelli, D. Maio, and D. Maltoni, "Semi-automatic enhancement of very low quality fingerprints," in *Proc. Int. Symp. Image Signal Process. Anal.*, 2009, pp. 678–683.
- [9] S. Chikkerur, A. N. Cartwright, and V. Govindaraju, "Fingerprint enhancement using STFT analysis," *Pattern Recognit.*, vol. 40, no. 1, pp. 198–211, 2007.
- [10] S. Yoon, J. Feng, and A. K. Jain, "On latent fingerprint enhancement," in *Biometric Technology for Human Identification VII*, Bellingham, WA, USA: SPIE, 2010.
- [11] S. Yoon, J. Feng, and A. K. Jain, "Latent fingerprint enhancement via robust orientation field estimation," in *Proc. Int. Joint Conf. Biometrics*, 2011, pp. 1–8.
- [12] J. Feng, J. Zhou, and A. K. Jain, "Orientation field estimation for latent fingerprint enhancement," *IEEE Trans. Pattern Anal. Mach. Intell.*, vol. 35, no. 4, pp. 925–940, Apr. 2013.
- [13] X. Yang, J. Feng, and J. Zhou, "Localized dictionaries based orientation field estimation for latent fingerprints," *IEEE Trans. Pattern Anal. Mach. Intell.*, vol. 36, no. 5, pp. 955–969, May 2014.
- [14] J. Zhang, R. Lai, and C.-C. J. Kuo, "Latent fingerprint segmentation with adaptive total variation model," in *Proc. Int. Conf. Biometrics*, 2012, pp. 189–195.
- [15] J. Zhang, R. Lai, and C.-C. J. Kuo, "Adaptive directional total-variation model for latent fingerprint segmentation," *IEEE Trans. Inf. Forensics Secur.*, vol. 8, no. 8, pp. 1261–1273, Aug. 2013.
- [16] K. Cao, E. Liu, and A. K. Jain, "Segmentation and enhancement of latent fingerprints: A coarse to fine ridgestructure dictionary," *IEEE Trans. Pattern Anal. Mach. Intell.*, vol. 36, no. 9, pp. 1847–1859, Sep. 2014.
- [17] M. Liu, X. Chen, and X. Wang, "Latent fingerprint enhancement via multi-scale patch based sparse representation," *IEEE Trans. Inf. Forensics Secur.*, vol. 10, no. 1, pp. 6–15, Jan. 2015.
- [18] K. Cao and A. K. Jain, "Latent orientation field estimation via convolutional neural network," in *Proc. Int. Conf. Biometrics*, 2015, pp. 349–356.
- [19] Y. Tang, F. Gao, J. Feng, and Y. Liu, "FingerNet: An unified deep network for fingerprint minutiae extraction," in *Proc. IEEE Int. Joint Conf. Biometrics*, 2017, pp. 108–116.
- [20] D.-L. Nguyen, K. Cao, and A. K. Jain, "Robust minutiae extractor: Integrating deep networks and fingerprint domain knowledge," in *Proc. Int. Conf. Biometrics*, 2018, pp. 9–16.
- [21] J. Svoboda, F. Monti, and M. M. Bronstein, "Generative convolutional networks for latent fingerprint reconstruction," in *Proc. IEEE Int. Joint Conf. Biometrics*, 2017, pp. 429–436.
- [22] J. Li, J. Feng, and C.-C. J. Kuo, "Deep convolutional neural network for latent fingerprint enhancement," *Signal Process.: Image Commun.*, vol. 60, pp. 52–63, 2018.
- [23] P. Qian, A. Li, and M. Liu, "Latent fingerprint enhancement based on DenseUNet," in *Proc. Int. Conf. Biometrics*, 2019, pp. 1–6.
- [24] K. Horapong, K. Srisutheanon, and V. Areekul, "Progressive latent fingerprint enhancement using two-stage spectrum boosting with matched filter and sparse autoencoder," in *Proc. Int. Conf. Elect. Eng./Electron. Comput. Telecommun. Inf. Technol.*, 2020, pp. 531–534.
- [25] M. Liu and P. Qian, "Automatic segmentation and enhancement of latent fingerprints using deep nested unets," *IEEE Trans. Inf. Forensics Secur.*, vol. 16, pp. 1709–1719, 2020.
- [26] A. Dabouei, S. Soleymani, H. Kazemi, S. M. Iranmanesh, J. Dawson, and N. M. Nasrabadi, "ID preserving generative adversarial network for partial latent fingerprint reconstruction," in *Proc. IEEE Int. Conf. Biometrics Theory Appl. Syst.*, 2018, pp. 1–10.
- [27] I. Joshi, A. Anand, M. Vatsa, R. Singh, S. D. Roy, and P. Kalra, "Latent fingerprint enhancement using generative adversarial networks," in *Proc. IEEE Winter Conf. Appl. Comput. Vis.*, 2019, pp. 895–903.
- [28] P. Q. Xijie Huang and M. Liu, "Latent fingerprint image enhancement based on progressive generative adversarial network," in *Proc. IEEE/CVF Conf. Comput. Vis. Pattern Recognit.*, 2020, pp. 8000–801.
- [29] ISO Central Secretary, "ISO/IEC JTC 1/SC 37 Biometrics," International Organization for Standardization, Standard ISO/IEC TR 19794–2:2011, 2011. [Online]. Available: <https://www.iso.org/committee/313770.html>
- [30] S. Reed, Z. Akata, X. Yan, L. Logeswaran, B. Schiele, and H. Lee, "Generative adversarial text to image synthesis," in *Proc. Int. Conf. Mach. Learn.*, 2016, pp. 1060–1069.
- [31] P. Isola, J.-Y. Zhu, T. Zhou, and A. A. Efros, "Image-to-image translation with conditional adversarial networks," in *Proc. IEEE Conf. Comput. Vis. Pattern Recognit.*, 2017, pp. 1125–1134.
- [32] I. Goodfellow et al., "Generative adversarial nets," in *Proc. Adv. Neural Inf. Process. Syst.*, 2014, pp. 2672–2680.
- [33] R. A. Yeh, C. Chen, T. Yian Lim, A. G. Schwing, M. Hasegawa-Johnson, and M. N. Do, "Semantic image inpainting with deep generative models," in *Proc. IEEE Conf. Comput. Vis. Pattern Recognit.*, 2017, pp. 5485–5493.
- [34] A. Buades, T. M. Le, J. M. Morel, and L. A. Vese, "Fast cartoon + texture image filters," *IEEE Trans. Image Process.*, vol. 19, no. 8, pp. 1978–1986, Aug. 2010.

- [35] O. Ronneberger, P. Fischer, and T. Brox, "U-Net: Convolutional networks for biomedical image segmentation," in *Proc. Int. Conf. Med. Image Comput. Comput.-Assist. Intervention*, 2015, pp. 234–241.
- [36] B. AlBahar and J.-B. Huang, "Guided image-to-image translation with bi-directional feature transformation," in *Proc. IEEE/CVF Int. Conf. Comput. Vis.*, 2019, pp. 9016–9025.
- [37] D. Pathak, P. Krahenbuhl, J. Donahue, T. Darrell, and A. A. Efros, "Context encoders: Feature learning by inpainting," in *Proc. IEEE Conf. Comput. Vis. Pattern Recognt.*, 2016, pp. 2536–2544.
- [38] Y. Wang, J. Hu, and D. Phillips, "A fingerprint orientation model based on 2D fourier expansion (FOMFE) and its application to singular-point detection and fingerprint indexing," *IEEE Trans. Pattern Anal. Mach. Intell.*, vol. 29, no. 4, pp. 573–585, Apr. 2007.